Original Article

Utility of FET-PET in detecting high-grade gliomas presenting with equivocal MR imaging features

ABSTRACT

High-grade gliomas, metastases, and primary central nervous system lymphoma (PCNSL) are common high-grade brain lesions, which may have overlapping features on magnetic resonance (MR) imaging. Our objective was to assess the utility of 18-fluoride-fluoro-ethyl-tyrosine positron emission tomography (FET-PET) in reliably differentiating between these lesions, by studying their metabolic characteristics. Patients with high-grade brain lesions suspicious for glioma, with overlapping features for metastases and PCNSL were referred for FET-PET by Neuroradiologists from Multidisciplinary Neuro-Oncology Joint Clinic. Tumor-to-contralateral white mater ratio (T/Wm) at 5 and 20 min was derived and compared to histopathology. Receiver operating characteristic curve analysis was used to find the optimal T/Wm cutoff to differentiate between the tumor types. T/Wm was higher for glial tumors compared to nonglial tumors (metastases, PCNSL, tuberculoma, and anaplastic meningioma). A cutoff of 1.9 was derived to reliably diagnose a tumor of glial origin with a sensitivity and specificity of 93.8% and 91%, respectively. FET-PET can be used to diagnose glial tumors presenting as high-grade brain lesions when MR findings show overlapping features for other common high-grade lesions.

Keywords: Brain lesions, fluoroethyl-tyrosine-positron-emission tomography, high-grage glioma, magnetic resonance imaging

INTRODUCTION

Contrast-enhanced magnetic resonance imaging (MRI) is the diagnostic modality of choice for characterizing brain neoplasms.[1] High-grade gliomas (HGGs), brain metastases (BM), and primary central nervous system lymphomas (PSNCL) are common high-grade brain malignancies in adults.[2] Contrast enhancement on T1-weighted images reflects areas of blood-brain barrier breakdown regardless of the pathology.[3] Advanced MR sequences, such as diffusion-weighted and perfusion imaging, are helpful; however, there still remains a subset of patients with imaging overlap.[4] Accurate preoperative diagnosis is often crucial because the management and prognosis of these tumors are substantially different. 18F-fluoroethyl-tyrosine (FET) is transported through L-amino acid transporters (LAT), which are present in normal brain parenchyma; and their expression proportionately increases with grade of glial proliferation.[5] It has been, thereby accepted as standard-of-care for differentiating between high-grade

and low-grade glial tumors.[6] Since all three conditions mentioned above have altogether different management plans, there is an unmet need for a noninvasive modality for differentiating between these lesions. FET-positron-emission tomography (FET-PET) has the potential to specifically detect glial tumors using semi-quantitative parameters;[7] hence, we

Ameya D. Puranik, Mathew Boon, Nilendu Purandare, Venkatesh Rangarajan, Tejpal Gupta[1], Aliasgar Moiyadi[2], Prakash Shetty[2], Epari Sridhar[3], Archi Agrawal, Indraja Dev, Sneha Shah

Departments of Nuclear Medicine and Molecular Imaging, [1]Radiation Oncology, [2]Neurosurgery and [3]Pathology, Tata Memorial Hospital, Homi Bhabha National University, Mumbai, Maharashtra, India

Address for correspondence: Dr. Ameya D. Puranik, Department of Nuclear Medicine and Molecular Imaging, Tata Memorial Hospital, Homi Bhabha National University, Mumbai, Maharashtra, India.
E-mail: ameya2812@gmail.com

Access this article online	
Website: www.wjnm.org	**Quick Response Code**
DOI: 10.4103/wjnm.WJNM_89_18	

conceptualized this study to generate reliable cut-off values by comparing the imaging findings with pathology.

MATERIALS AND METHODS

Patients

In this retrospective study design, we included 27 patients [Table 1], who presented with high-grade brain lesions (tumors belonging to Grades III and IV by the WHO classification of central nervous system [CNS]

Table 1: Patient Characteristics (G-Glioma, M-Metastases, L- Lymphoma)

Patient No	Age/Sex	Differentials on MR	T/Wm (5 min)	T/Wm (20 min)	Histopathology
1	55/M	G/M	2.2	2.3	Grade IV, Glioblastoma
2	58/M	G/L/M	2.04	2.2	Grade IV, Glioblastoma
3	55/F	G/L	2.6	2.2	Grade IV, Glioblastoma
4	38/F	G/L	2	2.2	Grade IV, Glioblastoma
5	21/F	G/L	1.2	1.1	Tuberculoma
6	62/M	G/M	1.8	1.1	Grade IV, Glioblastoma
7	54/M	G/L/M	1.6	1.6	Metastases
8	86/M	G/L	2.6	2.6	Grade IV, Glioblastoma
9	62/M	G/L	2.8	2.6	Grade IV, Glioblastoma
10	57/M	G/L/M	2.7	2.6	Grade IV, Glioblastoma
11	43/F	G/M	1.5	1.6	Metastases
12	78/M	G/L/M	2.4	2.5	Grade IV, Glioblastoma
13	67/F	G/L	1.3	1.4	PCNSL
14	35/M	G/L	1.8	1.6	Metastases
15	42/F	G/L/M	1.4	1.6	Grade III, Anaplastic meningioma
16	56/M	G/L/M	2.3	2.5	Grade IV, Glioblastoma
17	72/M	G/L/M	2.6	2.4	Grade IV, Glioblastoma
18	50/F	G/L/M	2.1	2.2	Grade IV, Glioblastoma
19	28/F	G/L/M	1.5	1.7	PCNSL
20	34/M	G/L/M	1.6	1.6	Tuberculoma
21	81/M	G/M	2.4	2.5	Grade IV, Glioblastoma
22	64/M	G/L	2.1	2.5	Grade IV, Glioblastoma
23	56/M	G/M	2.1	2.0	Metastases
24	48/F	G/L	1.6	1.8	PCNSL
25	45/M	G/L/M	2.8	2.7	Grade IV, Glioblastoma
26	72/M	G/L/M	1.2	1.5	Metastases
27	65/F	G/M	2.4	2.4	Grade IV , Glioblastoma

tumors – 2016 were defined as "high grade") on index MRI, between October 2016 and October 2017, which showed overlapping features for HGG and metastases, HGG and PCNSL, or for all the three tumor types [Table 2]. These findings were confirmed by two expert neuroradiologists, part of Multidisciplinary Neuro-Oncology Joint Clinic of our Institution, who thereafter advised FET-PET. These patients underwent FET-PET before any therapeutic interventions that might have influenced 18F-FET uptake in the tissue (surgery, biopsy, chemoradiotherapy, or radiosurgery). Furthermore, these patients underwent stereotactic biopsy or open resection within 6 weeks after MR and PET imaging, thus providing definite neuropathological diagnosis. This study design was approved by the Institutional Review Board and Ethics Committee of our Institution (Hospital IRB No – 3075).

Positron-emission tomography imaging

18F-FET was manufactured at in-house medical cyclotron facility. PET studies were acquired after intravenous injection of 222–296 MBq of 18F-FET using dedicated PET/computed tomography (CT) scanners (Philips Astonish Time-of-Flight systems) incorporating 16-slice and 64-slice CT components, respectively. Static acquisition was performed by acquiring limited images with brain in field-of-view at 5 min and 20 min, each for the duration of 5 min.

Image processing

Images were processed and reported by one nuclear medicine physician who was blinded to clinical history and MR findings. Tumor-to-contralateral white mater ratio (T/Wm) was the semi-quantitative parameter used for image analysis. Transaxial slices showing the highest 18F-FET accumulation in the tumors were chosen for the region of interest (ROI) analyses. Three-dimensional volumetric ROI was placed on axial, coronal, and sagittal planes by the nuclear medicine physician [Figure 1]. Maximum standardized uptake value (SUV_{max}) at the tumor site was derived. Another ROI was placed over contralateral white mater over three consecutive slices, and average of these values was taken as SUV_{max} over contralateral white mater. T/Wm was calculated by dividing the above two parameters (SUV_{max} of tumor and contralateral white mater). All primary brain lesions were subjected to a surgical biopsy or resection for histopathological confirmation. Receiver operating characteristic curve analysis was used to find the optimal T/Wm value that could differentiate glial tumors from other pathologies.

RESULTS

Table 1 shows the demographic details, MR findings, FET-PET findings, and histopathological results in all patients. This study included 27 patients (male/female: 17/10), with a median

## Table 2: MR imaging features (G-Glioma, M-Metastases, L- Lymphoma)

Patient No	MR diagnosis	MR findings				
		Location	T2 intensity	Post Contrast	Spectroscopy	Perfusion
1	G/M	Left temporal	Hypo	Enhancing	Choline Peak	Hypoperfused
2	G/L/M	Peri-ventricular	Hypo	Enhancing	Choline Peak	Hyperperfused
3	G/L	Left insular	Hyper	Ring-enhancing	Choline peak	Hyperperfused
4	G/L	Peri-ventricular	Hypo	Enhancing	Choline peak	Hypoperfused
5	G/L	Grey-white interface	Central Hypo	Ring-enhancing	Non-contributory	Mild hyperperfusion
6	G/M	Midline pericallosal	Iso-	Enhancing	Choline Peak	Hypoperfused
7	G/L/M	Right frontal	Iso	Ring-enhancing	Non-contributory	Hyperperfused
8	G/L	Right frontal	Hypo	Ring-enhancing	Non-contributory	Hyperperfused
9	G/L	Periventricular	Iso to hyper	Ring-enhancing	Choline peak	Mild hyperperfusion
10	G/L/M	Left medial temporal	Hypo	Enhancing	Choline peak	Hypoperfused
11	G/M	Right parietal	Hypo	Ring-enhancing	Non-contributory	Hyperperfused
12	G/L/M	Left parieto-temporal	Iso	Ring-enhancing	Non-contributory	Hyperperfused
13	G/L	Peri-ventricular	Hypo	Enhancing	Choline peak	Hypoperfused
14	G/L	Left Temporal	Hypo	Ring-enhancing	Non-contributory	Hyperperfused
15	G/L/M	Left frontal	Iso to hyper	Enhancing	Non-contributory	Hyperperfused
16	G/L/M	Left temporal	Hypo	Enhancing	Choline Peak	Hypoperfused
17	G/L/M	Right insular	Hypo	Enhancing	Non-contributory	Hypoperfused
18	G/L/M	Left frontal	Hypo	Ring-enhancing	Non-contributory	Hypoperfused
19	G/L/M	Periventricular	Iso to hyper	Ring-enhancing	Choline peak	Hyperperfused
20	G/L/M	Left Temporal	Hypo	Ring-enhancing	Non-contributory	Hyperperfused
21	G/M	Peri-ventricular	Hypo	Enhancing	Choline peak	Hypoperfused
22	G/L	Left insular	Hyper	Ring-enhancing	Non-contributory	Hyperperfused
23	G/M	Right parietal	Hypo	Ring-enhancing	Non-contributory	Hyperperfused
24	G/L	Periventricular	Iso	Ring-enhancing	Choline peak	hyperperfused
25	G/L/M	Right frontal	Iso to hyper	Ring-enhancing	Non-contributory	Hypoperfused
26	G/L/M	Left frontal	Hypo	Ring-enhancing	Non-contributory	Hyperperfused
27	G/M	Right temporal	Iso	Ring-enhancing	Choline Peak	Hypoperfused

Iso- Iso-intense, Hypo-hypointense, hyper-hyperintense
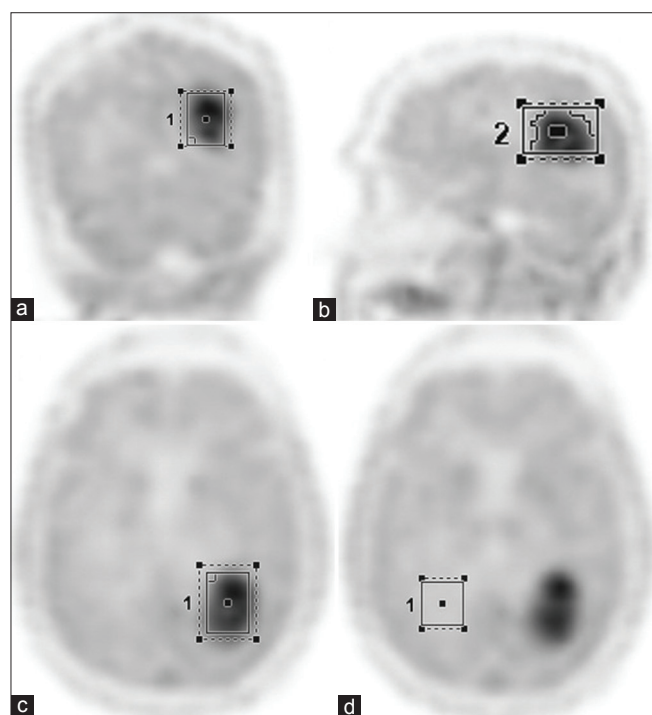
Figure 1: Region of interest generated over coronal (a), sagittal (b), and axial (c) FET-PET images. Background region of interest drawn over contralateral white mater (d) on axial PET image

age of 56 years (range: 21–86 years). Based on MRI findings, radiological differentials were HGG and PCNSL in nine patients [Figures 2 and 3], HGG and metastases in five patients [Figure 4], and all three differentials (HGG, PCNSL, and metastases) in 13 patients [Figure 5]. On final histopathology, 16 patients were diagnosed with HGG, five with metastases, and three with PCNSL. Two patients had tuberculoma and one had anaplastic meningioma. PCNSL had a low T/Wm (mean of 1.46 at 5 min and 1.63 at 20 min); metastases also had a low T/Wm (mean of 1.64 and 1.66 at 5 and 20 min, respectively). Similarly, other three patients with tuberculoma (mean T/Wm 1.4 and 1.35 at 5 and 20 min) and anaplastic meningioma (T/Wm – 1.4 and 1.6 at 5 and 20 min) had low T/Wm. However, HGG, all of which were diagnosed as Grade 4 on final histopathology, showed a relatively higher T/Wm with a mean of 2.36 and 2.33 at 5 and 20 min, respectively. Thus, all high-grade nonglial tumors showed a mean T/Wm of 1.52 at 5 min and 1.59 at 20 min, which was significantly lower compared to high-grade tumors of glial origin [Figure 6]. T/Wm cutoff of 1.9 at both 5 min and 20 min showed 93.8% sensitivity [Figure 7] and 91% specificity to diagnose HGGs; (5 min – area under the curve (AUC) =0.974, $P = 0.00$, 20 min AUC = 0.940, $P = 0.00$).
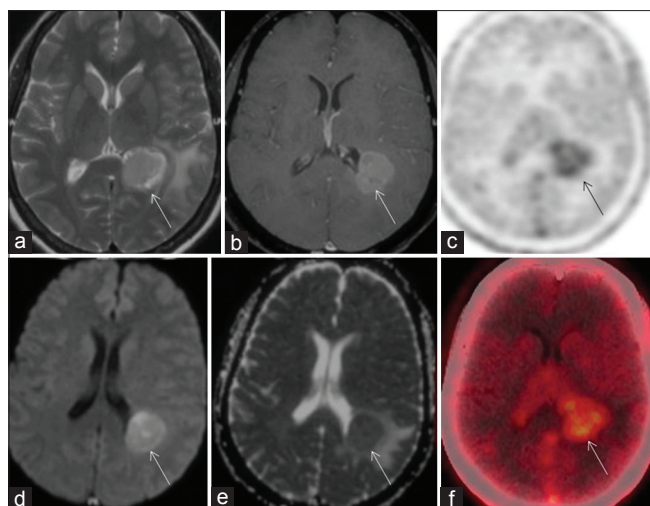
Figure 2: Patient 3 was a 55-year-old female, presented with headache for 1 month, axial MR sequences (arrows) show well-circumscribed mass along the occipital horn of left lateral ventricle, (a) iso-to-hypointense on T2-weighted image (b) enhancing on postcontrast T1-weighted image, with (d) restricted diffusion and (e) low apparent diffusion coefficient, hyperperfusion on MR perfusion sequence; MR spectroscopy was noncontributory. Although features were favoring PCNSL, age and rapid clinical deterioration raised the suspicion of glial tumor. Axial FET-PET (c and f) fused PET/CT images (arrows) showed increased tracer uptake in the mass, with a tumor-to-contralateral white mater ratio of 2.6 and 2.2 at 5 and 20 min. Biopsy was suggestive of the WHO Grade IV glioma – glioblastoma

DISCUSSION

PCNSL, metastases, and HGG are the three most common differentials for high-grade intracranial lesions seen in clinical practice. Accurate differentiation is of high value as the management protocols and prognosis for each of three conditions is altogether different.[8-10] The objective of this study, therefore, was to assess the utility of FET-PET in detecting HGGs, when lesions did not demonstrate classical MRI features, in spite of high index of suspicion. Since we included just those patients who had equivocal MRI studies in spite of advanced sequences, the sample size was limited to 27 patients. We generated a cutoff of 1.9 for tumor-to-white matter ratio on FET-PET to distinguish between glial and nonglial lesions. Nonglial lesions included BM, PCNSL, two tuberculomas, and one anaplastic meningioma. Out of four patients with BM, two had primary in the lung, one as anorectal melanoma, and one in the breast. FET-PET, with a sensitivity and specificity of 93% and 91%, respectively, for diagnosing HGGs, has shown potential to be used in this clinical situation.

A meta-analysis by Dunet *et al*.,[11] derived maximum tumor-to-background ratio (TBRmax) cutoff of 2.1 for differentiating glial and nonglial tumors. However, it had a modest sensitivity and specificity of 71% and 72%, primarily because gliomas across all grades were included in the study. Most studies using FET-PET have focused on its utility in
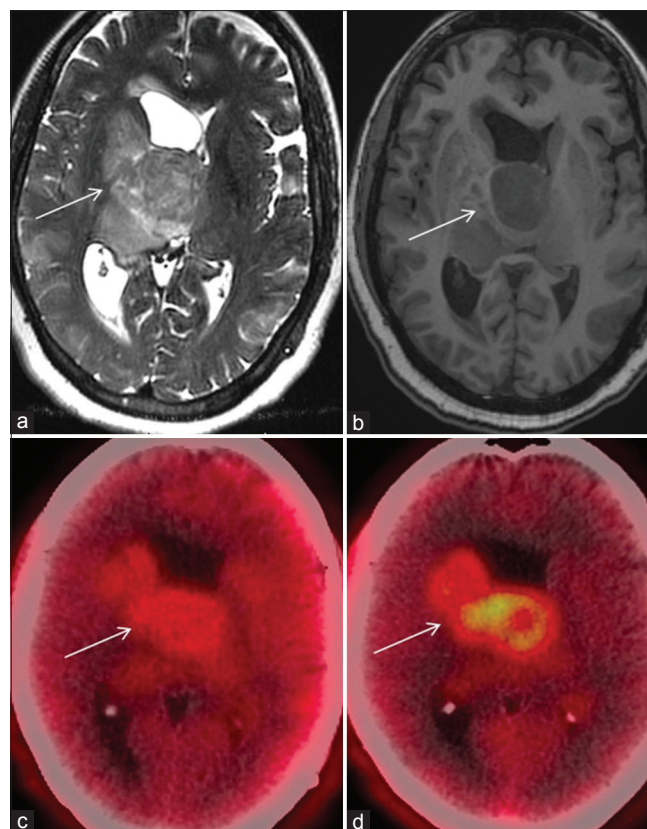
Figure 3: An 86-year-old male (patient 8), known case of chronic kidney disease, presenting with headache and limb weakness, underwent a MRI at a regional center; axial images (a) showed an ill-defined T1 hypointense, T2 iso-to-hypointense corpus callosal lesion infiltrating the ventricles and right thalamus, no contrast could be administered, there was facilitated diffusion on diffusion-weighted imaging and ADC map; hyperperfusion on MR perfusion images differentials of PCNSL and high-grade glioma were given. FET-PET showed tumor-to-contralateral white mater (T/Wm) ratio of 2.6 on both 5 (c) and 20 (d) minute images. 5-min image is an index of vascularity, however, since maximum uptake occurs till 20 min, increased 20-min uptake in the hyperperfused lesions seen at 5 min is suggestive of high-grade glioma. Histopathology revealed Grade IV gliomas

grading gliomas.[12] Conventional MRI has similar accuracy,[13] for this purpose and recent literature with advanced magnetic resonance (MR) techniques have shown higher accuracy and specificity.[14] This obviates the need for additional molecular imaging for grading of gliomas. However, for undiagnosed brain lesions, MR features are not always confirmatory. MRI findings of tumor infiltration and contrast enhancement can be seen in all three high-grade tumors. Diffusion-weighted imaging which is an index of cellularity of tumor may be nonspecific in some cases.[15] Relative cerebral blood volume, a parameter on MR perfusion imaging, which offers the highest accuracy for distinguishing glioblastoma, metastases, and PCNSLs,[16] has remarkable sensitivity but has modest specificity of 64%.[17]

There have been studies with fluorodeoxyglucose (FDG) PET for characterizing high-grade lesions. Purandare *et al*.
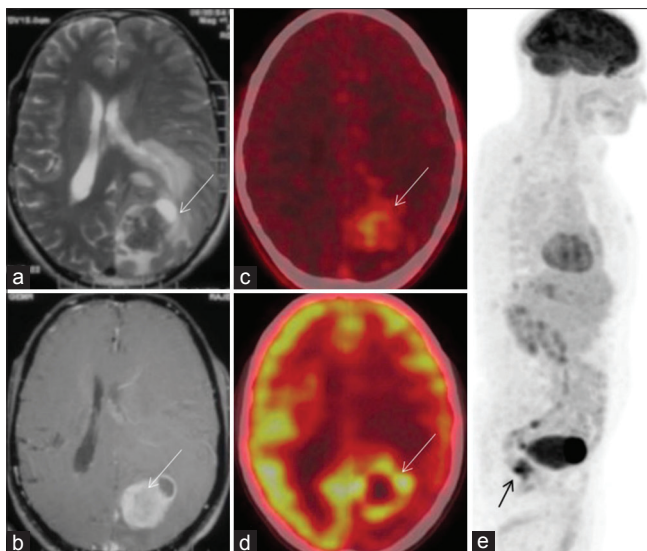
Figure 4: Patient 7 is a 54-year-old male, presented with progressive bilateral diminution of vision and right hemiparesis for 2 months, MRI showed (a) T2-hypointense lesion in the left occipital region, with perilesional edema. (b) Axial postcontrast T1-weighted image showed homogeneous enhancement. MR spectroscopy and perfusion were noncontributory. Differentials were high-grade glioma, PCNSL with rare possibility of metastases. FET-PET was done (c), which showed low-grade uptake in the lesion with a tumor-to-contralateral white mater (T/Wm) ratio of 1.6 at 5 and 20 min. Patient was not willing for biopsy; hence, whole-body FDG PET was done which showed rim of increased uptake in the brain lesion ([d] equal to gray matter), and primary site in the anal canal, seen on maximum intensity projection (MIP) image ([e] – arrow), biopsy showed anal melanoma, thus brain lesion was most likely metastatic. FET-PET (T/Wm) ratio was useful in ruling out high-grade glioma

showed no difference in SUV_{max} values for HGG and BM whereas SUV_{max} of 15.5 showed sensitivity and specificity of 84% and 80% for diagnosing PCNSL.[18] Two similar studies have shown the similar cutoff for detecting PCNSL, but false positives have been reported, owing to lack of specificity.[19,20] The need of specific tracer is important since not all lesions are amenable to biopsy, and treatment plans are based on imaging diagnosis. Radiolabeled amino acids such as methionine and FET show selectively high uptake in proliferating glial tissue but low uptake in normal brain tissue. FET uptake significantly correlates with tumor cell density and proliferation rate as well as with microvascular density and neoangiogenesis; all of these being pathological markers of HGGs.[21] FET is not incorporated into metabolic pathway, and uptake is directly proportional to the density of LAT-2; which is overexpressed on proliferating glial cells and not present on inflammatory cell or other tumor types, making it specific for HGGs. FET localization is independent of the integrity of blood–brain barrier, thus nonenhancing lesions on MR can be characterized.[22] Another important aspect is the impact of steroid on the uptake of FET. Unlike FDG-PET, in which uptake could be influenced by cumulative doses of corticosteroid before a PET scan, steroids do not significantly impact TBR values in FET-PET.[23,24] Unlike existing literature that proposes a dynamic imaging protocol, we preferred dual-point static
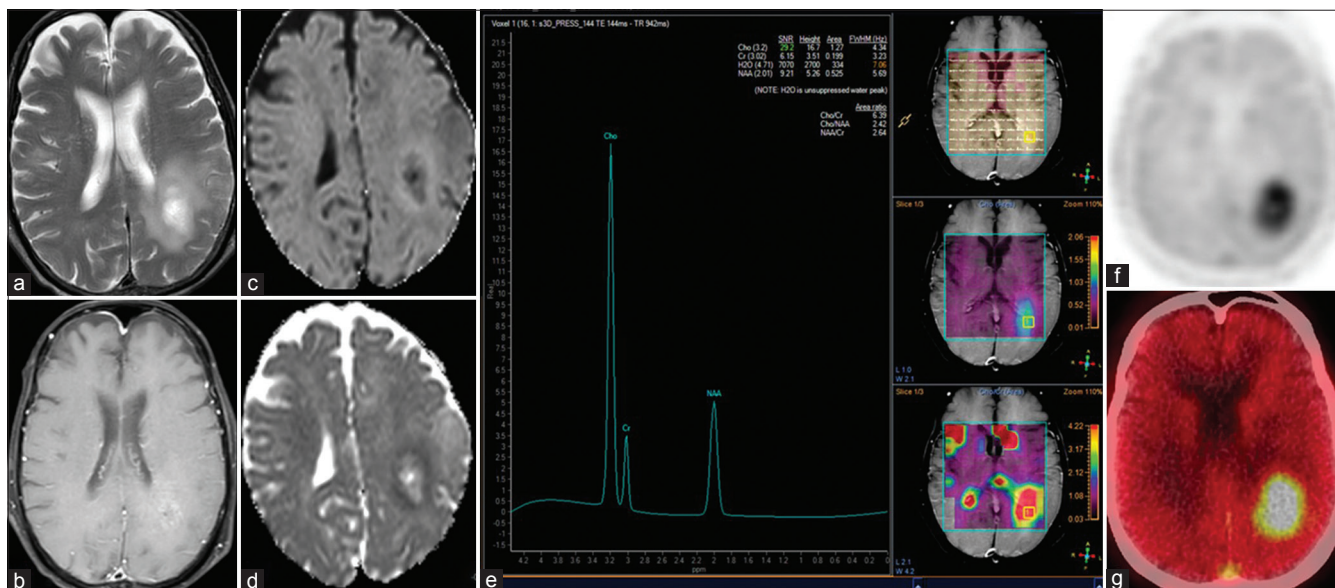
Figure 5: Patient 12 was a 78-year-old male presented with memory loss, MRI showed well-defined lesion in the left parietal region (arrows), periventricular location, (a) hyperintense on T2 with edema, (b) T1-postcontrast showed minimal enhancement, (c and d) rim of restricted diffusion and low apparent diffusion coefficient, (e) MR spectroscopy showed choline peak with raised Cho/Cr ratio, and MR perfusion imaging showed relative cerebral blood volume of 158.3 suggestive of mild hyperperfusion. Considering the age and overlapping imaging features, differentials of PCNSL, metastases, and high-grade glioma were given. FET-PET showed intense uptake in lesion on axial PET (f) and fused PET/CT (g) images with tumor-to-contralateral white mater (T/Wm) ratio of 2.4 and 2.5 at 5 and 20 min, favoring high-grade glioma. Histopathology was WHO Grade IV glioma – glioblastoma
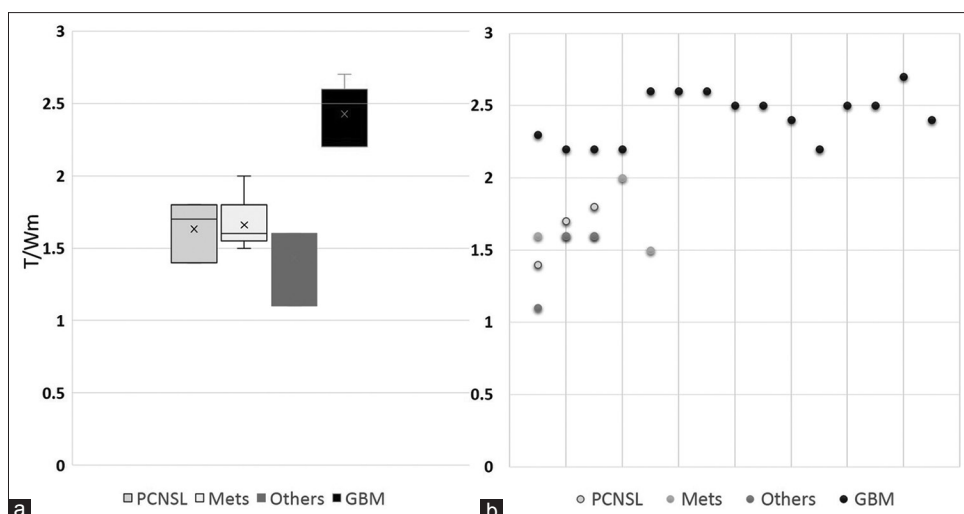
Figure 6: (a) Box plot and (b) dot plot depicting the tumor-to-white matter (T/Wm) ratio across PCNSL, metastases, glioblastoma, and other lesions
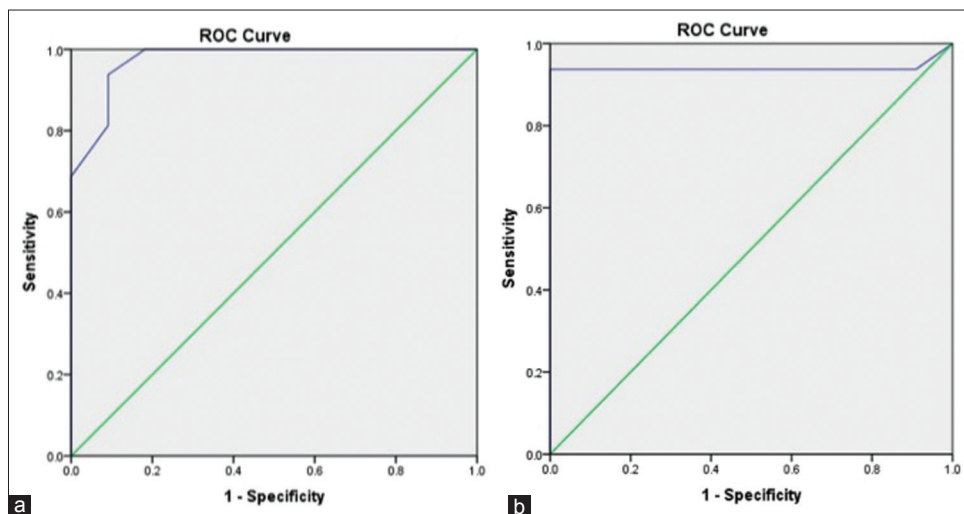

Figure 7: Area under the curve showing a 1.9 tumor-to-white matter (T/Wm) ratio cutoff to differentiate high-grade glial and nonglial high-grade lesions with a sensitivity of 93.8% and specificity of 91%, at 5 min (a) and 20 min (b). ROC: Receiver operating characteristic

acquisition (5 and 20 min), based on the study by Albert *et al*.[25] Peak FET concentration in glial tumors occurs approximately at 20 min and declines slightly thereafter. 5-min image was acquired to assess the tumor perfusion, which shows an early peak in HGGs, with a small subset of lesions showing overestimation of FET uptake in early images due to high vascularity.[26] Static 20-min image helps to confirm the findings on 5-min image as well as provides tumor extent. In addition, static acquisition improved patient compliance with shorter scanning time, avoiding motion artifacts. It led to reduction of scanning time per patient, which is crucial for high-volume PET/ CT departments.

Rapp *et al*.[27] derived a TBRmax cutoff of 2.5 to differentiate gliomas from other brain lesions. However, the clinical benefit was unclear as it included all brain lesions,

including high- and low-grade gliomas, which brought down the sensitivity to 57%. Since molecular imaging using PET involves target-specific tracers, the clinical question that is to be answered is of utmost importance. Our study was thereby designed to address a practical clinical issue faced in neuro-oncology clinic of a large tertiary care hospital. The retrospective nature and small cohort are the limitations; however, with the results of this study, a larger prospective study can be designed to generate more robust results.

CONCLUSION

FET-PET has shown potential to become the modality of choice for detecting high-grade glial tumors from other high-grade brain lesions when the MRI features are equivocal.

REFERENCES

1. Chen W, Silverman DH. Advances in evaluation of primary brain tumors. Semin Nucl Med 2008;38:240-50.
2. Ostrom QT, Gittleman H, Liao P, Vecchione-Koval T, Wolinsky Y, Kruchko C, *et al*. CBTRUS Statistical Report: Primary Brain and Other Central Nervous System Tumors Diagnosed in the United States in 2010–2014. Neuro Oncol 2017;19:iv1-iv88.
3. Price SJ. The role of advanced MR imaging in understanding brain tumour pathology. Br J Neurosurg 2007;21:562-75.
4. Ding Y, Xing Z, Liu B, Lin X, Cao D. Differentiation of primary central nervous system lymphoma from high-grade glioma and brain metastases using susceptibility-weighted imaging. Brain Behav 2014;4:841-9.
5. Langen KJ, Stoffels G, Filss C, Heinzel A, Stegmayr C, Lohmann P, *et al*. Imaging of amino acid transport in brain tumours: Positron emission tomography with O-(2-[18F]fluoroethyl)-L-tyrosine (FET). Methods 2017;130:124-34.
6. la Fougère C, Suchorska B, Bartenstein P, Kreth FW, Tonn JC. Molecular imaging of gliomas with PET: Opportunities and limitations. Neuro Oncol 2011;13:806-19.
7. Floeth FW, Pauleit D, Sabel M, Reifenberger G, Stoffels G, Stummer W, *et al*. 18F-FET PET differentiation of ring-enhancing brain lesions. J Nucl Med 2006;47:776-82.
8. Omuro A, DeAngelis LM. Glioblastoma and other malignant gliomas: A clinical review. JAMA 2013;310:1842-50.
9. Sperduto PW, Chao ST, Sneed PK, Luo X, Suh J, Roberge D, *et al*. Diagnosis-specific prognostic factors, indexes, and treatment outcomes for patients with newly diagnosed brain metastases: A multi-institutional analysis of 4,259 patients. Int J Radiat Oncol Biol Phys 2010;77:655-61.
10. Pasricha S, Gupta A, Gawande J, Trivedi P, Patel D. Primary central nervous system lymphoma: A study of clinicopathological features and trend in Western India. Indian J Cancer 2011;48:199-203.
11. Dunet V, Rossier C, Buck A, Stupp R, Prior JO. Performance of 18F-fluoro-ethyl-tyrosine (18F-FET) PET for the differential diagnosis of primary brain tumor: A systematic review and metaanalysis. J Nucl Med 2012;53:207-14.
12. Gempt J, Bette S, Ryang YM, Buchmann N, Peschke P, Pyka T, *et al*. 18F-fluoro-ethyl-tyrosine positron emission tomography for grading and estimation of prognosis in patients with intracranial gliomas. Eur J Radiol 2015;84:955-62.
13. Verger A, Filss CP, Lohmann P, Stoffels G, Sabel M, Wittsack HJ, *et al*. Comparison of 18F-FET PET and perfusion-weighted MRI for glioma grading: A hybrid PET/MR study. Eur J Nucl Med Mol Imaging 2017;44:2257-65.
14. Rizzo L, Crasto SG, Moruno PG, Cassoni P, Rudà R, Boccaletti R, *et al*. Role of diffusion- and perfusion-weighted MR imaging for brain tumour characterisation. Radiol Med 2009;114:645-59.
15. Kono K, Inoue Y, Nakayama K, Shakudo M, Morino M, Ohata K, *et al*. The role of diffusion-weighted imaging in patients with brain tumors. AJNR Am J Neuroradiol 2001;22:1081-8.
16. Hartmann M, Heiland S, Harting I, Tronnier VM, Sommer C, Ludwig R, *et al*. Distinguishing of primary cerebral lymphoma from high-grade glioma with perfusion-weighted magnetic resonance imaging. Neurosci Lett 2003;338:119-22.
17. Blasel S, Jurcoane A, Franz K, Morawe G, Pellikan S, Hattingen E, *et al*. Elevated peritumoural rCBV values as a mean to differentiate metastases from high-grade gliomas. Acta Neurochir (Wien) 2010;152:1893-9.
18. Purandare NC, Puranik A, Shah S, Agrawal A, Gupta T, Moiyadi A, *et al*. Common malignant brain tumors: Can 18F-FDG PET/CT aid in differentiation? Nucl Med Commun 2017;38:1109-16.
19. Das K, Mittal BR, Vasistha RK, Singh P, Mathuriya SN. Role of (18) F-fluorodeoxyglucose positron emission tomography scan in differentiating enhancing brain tumors. Indian J Nucl Med 2011;26:171-6.
20. Kosaka N, Tsuchida T, Uematsu H, Kimura H, Okazawa H, Itoh H, *et al*. 18F-FDG PET of common enhancing malignant brain tumors. AJR Am J Roentgenol 2008;190:W365-9.
21. Stegmayr C, Schöneck M, Oliveira D, Willuweit A, Filss C, Galldiks N, *et al*. Reproducibility of O-(2-(18)F-fluoroethyl)-L-tyrosine uptake kinetics in brain tumors and influence of corticoid therapy: An experimental study in rat gliomas. Eur J Nucl Med Mol Imaging 2016;43:1115-23.
22. Yamaguchi S, Hirata K, Kobayashi H, Shiga T, Manabe O, Kobayashi K, *et al*. The diagnostic role of (18) F-FDG PET for primary central nervous system lymphoma. Ann Nucl Med 2014;28:603-9.
23. Pöpperl G, Kreth FW, Mehrkens JH, Herms J, Seelos K, Koch W, *et al*. FET PET for the evaluation of untreated gliomas: Correlation of FET uptake and uptake kinetics with tumour grading. Eur J Nucl Med Mol Imaging 2007;34:1933-42.
24. Langen KJ, Hamacher K, Weckesser M, Floeth F, Stoffels G, Bauer D, *et al*. O-(2-[18F]fluoroethyl)-L-tyrosine: Uptake mechanisms and clinical applications. Nucl Med Biol 2006;33:287-94.
25. Albert NL, Winkelmann I, Suchorska B, Wenter V, Schmid-Tannwald C, Mille E, *et al*. Early static (18)F-FET-PET scans have a higher accuracy for glioma grading than the standard 20-40 min scans. Eur J Nucl Med Mol Imaging 2016;43:1105-14.
26. Heiss P, Mayer S, Herz M, Wester HJ, Schwaiger M, Senekowitsch-Schmidtke R, *et al*. Investigation of transport mechanism and uptake kinetics of O-(2-[18F]fluoroethyl)-L-tyrosine *in vitro* and *in vivo*. J Nucl Med 1999;40:1367-73.
27. Rapp M, Heinzel A, Galldiks N, Stoffels G, Felsberg J, Ewelt C, *et al*. Diagnostic performance of 18F-FET PET in newly diagnosed cerebral lesions suggestive of glioma. J Nucl Med 2013;54:229-35.